cmgh
CELLULAR AND MOLECULAR GASTROENTEROLOGY AND HEPATOLOGY

ORIGINAL RESEARCH

Increased Bcl-xL Expression in Pancreatic Neoplasia Promotes Carcinogenesis by Inhibiting Senescence and Apoptosis

Kenji Ikezawa,[1] Hayato Hikita,[1] Minoru Shigekawa,[1] Kiyoshi Iwahashi,[1] Hidetoshi Eguchi,[2] Ryotaro Sakamori,[1] Tomohide Tatsumi,[1] and Tetsuo Takehara[1]

[1]Department of Gastroenterology and Hepatology, [2]Department of Gastroenterological Surgery, Osaka University Graduate School of Medicine, Suita, Japan

SUMMARY

Bcl-xL expression increased with the progression of pancreatic neoplasia from pancreatic intraepithelial neoplasia (PanIN)-1 to pancreatic ductal adenocarcinoma. Bcl-xL overexpression in low-grade PanINs inhibits oncogene-induced senescence, whereas it inhibits apoptosis in high-grade PanINs, accelerating carcinogenesis. Bcl-xL deficiency increased senescence in PanINs.

BACKGROUND & AIMS: Bcl-xL, an anti-apoptotic Bcl-2 family protein, is overexpressed in 90% of pancreatic ductal adenocarcinoma (PDAC) cases. However, Bcl-xL expression in pancreatic intraepithelial neoplasias (PanINs) and its significance in PDAC carcinogenesis remain unclear. The aim of this study was to elucidate the significance of Bcl-xL expression in PanINs.

METHODS: We investigated the expression levels of Bcl-xL in pancreas-specific KrasG12D (P-KrasG12D) mice and human PanINs and PDAC. We examined the impact of Bcl-xL expression on Kras-mutated pancreatic neoplasia using Bcl-xL–overexpressing P-KrasG12D mice and Bcl-xL–knockout P-KrasG12D mice.

RESULTS: In P-KrasG12D mice, the number of PanINs increased and their grades progressed with age. In total, 55.6% of these mice developed PDAC at 12–14 months. According to the immunohistochemistry of mouse pancreas and human resected specimens, Bcl-xL expression was increased significantly in PanIN-1 compared with that in normal pancreatic ducts, and augmented further with the progression of pancreatic neoplasia in PanIN-2/3 and PDAC. Oncogene-induced senescence was observed frequently in PanIN-1, but rarely was detected in PanIN-2/3 and PDAC. Bcl-xL overexpression significantly accelerated the progression to high-grade PanINs and PDAC and reduced the survival of P-KrasG12D mice. Bcl-xL overexpression in P-KrasG12D mice suppressed oncogene-induced senescence in PanIN-1 and inhibited apoptosis in PanIN-3. Bcl-xL deficiency in P-KrasG12D mice induced cellular senescence in PanIN-2/3.

CONCLUSIONS: Bcl-xL expression increases with the progression from PanIN-1 to PDAC, whereas oncogene-induced senescence decreases. Bcl-xL overexpression increases PDAC incidence rates by inhibiting oncogene-induced senescence and apoptosis in PanINs. Conversely, Bcl-xL deficiency induced senescence in PanINs. Anti–Bcl-xL treatments may have the potency to suppress the progression from PanINs to PDAC. *(Cell Mol Gastroenterol Hepatol 2017;4:185–200; http://dx.doi.org/10.1016/j.jcmgh.2017.02.001)*

Keywords: Kras; PanINs; Bcl-2 Family Protein.

Pancreatic ductal adenocarcinoma (PDAC) is one of the most highly aggressive forms of human cancer, with <5% of patients surviving after 5 years, and the early detection of PDAC remains difficult.[1,2] The number of patients with PDAC has increased steadily, and PDAC has increased to the fourth leading cause of cancer-related death in the United States.[3] Pancreatic intraepithelial neoplasias (PanINs) are the most frequent and well-characterized precursor lesions of PDAC.[4,5] PanINs are classified into PanIN-1, 2, and 3, depending on the degree of cytologic and architectural atypia.[6] Kras mutations, the most frequent genetic alteration of PDAC, are identified in more than 90% of low-grade PanIN-1/2, as well as high-grade PanIN-3 and PDAC in human beings.[7,8] A pancreas-specific Kras mutant mouse model, which develops PanINs and PDAC over time,[9] is suitable for studying both PanINs and PDAC.

Bcl-xL is one of the anti-apoptotic Bcl-2 family proteins.[10] Bcl-xL inhibits Bak or Bax activation, which is an essential event for apoptosis execution.[11,12] Previous reports have clarified that increased Bcl-xL expression is observed in 90% of PDAC cases based on immunohistochemical analysis using tumor tissues of PDAC patients.[13,14] However, the expression levels in PanINs remain unclear. The impact of Bcl-xL overexpression on PDAC carcinogenesis also remains uncharacterized.

In the present study, Bcl-xL expression showed a graded increase with the progression of pancreatic neoplasia from

Abbreviations used in this paper: **IHC, immunohistochemistry; KO, knockout; P-KrasG12D, Pdx1-Cre LSL-KrasG12D; PanIN, pancreatic intraepithelial neoplasia; PDAC, pancreatic ductal adenocarcinoma; SA–β-gal, senescence-associated β-galactosidase; siRNA, small interfering RNA; Tg, transgenic; TUNEL, terminal deoxynucleotidyl transferase–mediated deoxyuridine triphosphate nick-end labeling.**

Most current article

2352-345X
http://dx.doi.org/10.1016/j.jcmgh.2017.02.001

PanIN-1 to PDAC. Bcl-xL overexpression accelerated PDAC carcinogenesis with the decrease of senescence in PanIN-1 and apoptosis in PanIN-3, reducing survival in Kras mutant mice. Conversely, Bcl-xL deficiency induced senescence in PanINs. This study showed the function of Bcl-xL and its effect on the process of pancreatic carcinogenesis.

Materials and Methods

Genetically Engineered Mouse Models and Mouse Strains

The *Pdx1-Cre* transgenic (Tg) strain on a C57BL/6/FVB background and the *LSL-KrasG12D* knock-in strain on a C57BL/6/129 background were obtained from the Mouse Models of Human Cancer Consortium (National Cancer Institute–Frederick, Bethesda, Maryland). The LSL-KrasG12D allele is expressed at endogenous levels after Cre-mediated excision of a transcriptional stopper element.[9,15] A heterozygous hemagglutinin-hBcl-xL transgenic strain expressing the human Bcl-xL gene under the regulation of the CAG promoter on a C57BL/6/129 background (Bcl-xL Tg mice) using a hemagglutinin-tagged human Bcl-xL expression plasmid (pcDNA3HAbcl-xL) was described previously.[16] Mice carrying a *bcl-x* gene with 2 loxP sequences in the promotor region and a second intron (*bcl-x*$^{flox/flox}$ mice) were described previously.[17] These strains were intercrossed to produce the experimental cohorts. Mice were genotyped by polymerase chain reaction analysis (primer sequences are provided in the Supplementary Materials and Methods section). All mice were maintained with free access to food and water in a specific pathogen-free facility. They were treated with humane care under approval from the Animal Care and Use Committee of Osaka University Medical School.

Histologic Evaluation

Formalin-fixed, paraffin-embedded mouse pancreas tissues were sectioned (4 μm) and stained with H&E. PanIN lesions and carcinoma were classified according to histopathologic criteria.[18] To quantify the progression of PanIN lesions, the number and their grades from each sample were obtained from 10 high-power ($\times$200) microscopic fields. The area of normal-appearing pancreatic tissue was measured using the Hybrid Cell Count analysis of a digital microscope image (BZ-X700; Keyence, Osaka, Japan). Terminal deoxynucleotidyl transferase–mediated deoxyuridine triphosphate nick-end labeling (TUNEL) staining, which is used to detect apoptotic cells,[19,20] was performed as previously described.[21]

Immunohistochemistry

The sections of mouse pancreas were processed further for immunohistochemistry (IHC). The sections were immersed in 1$\times$ Target Retrieval Solution (pH 6.0) (Dako, Glostrup, Denmark) for Bcl-xL and p21 staining. The samples were heated to 120°C in a decloaking chamber for antigen retrieval. The endogenous peroxidase activity was quenched by incubating with 3% hydrogen peroxide in methanol for 30 minutes. After sections were blocked in 5% goat serum for 1 hour, they were incubated with antibodies against Bcl-xL (1:200, #2764; Cell Signaling Technology, Danvers, MA) and p21 (1:400, sc-471; Santa Cruz Biotechnology, Santa Cruz, CA) overnight at 4°C. After rinsing with phosphate-buffered saline, the slides were incubated with secondary antibody (SignalStain Boost IHC detection reagent; Cell Signaling Technology) for 30 minutes. After washes with phosphate-buffered saline, the sections were incubated with 3,3'-diaminobenzidine for 30 seconds and counterstained with hematoxylin. In every staining set, negative controls were applied by omission of the primary antibody.

Evaluation of the Immunohistochemistry Results

Immunohistochemical staining for Bcl-xL was defined as a detectable immunoreaction in the cytoplasm. The number of positive cells was estimated semiquantitatively. The quantity of the immunostaining was evaluated as follows: 0 corresponded to no positive immunostaining, 1 corresponded to less than 20%, 2 corresponded to 20%–75%, and 3 corresponded to more than 75% positive cells.[22] The intensity of the immunostaining was evaluated as follows: 0 corresponded to no staining, 1 corresponded to weak staining, 2 corresponded to moderate staining, and 3 corresponded to intense staining.[23] A combined total score for the immunostaining was calculated by adding both the quantitative score and the intensity score. The total score for each sample was the average score obtained from 10 high-power (magnification, $\times$200) microscopic fields.

Senescence-Associated β-Galactosidase Assay

To assess senescence in vivo, mouse pancreatic cryosections were stained for senescence-associated β-galactosidase (SA–β-gal) activity according to a previously described procedure.[24] Briefly, the frozen pancreas sections were fixed in 0.2% glutaraldehyde with 2% formaldehyde for 1 minute and incubated overnight in SA–β-gal solution from the Senescence β-Galactosidase Staining Kit (Cell Signaling Technology) at 37°C. This staining kit also was used for the evaluation of senescence in vitro according to the manufacturer's protocol. A total of approximately 500 cells was counted in 4 randomly selected fields to determine the percentage of senescent cells.

Human Samples

Formalin-fixed, paraffin-embedded samples were obtained from 9 patients with PDAC accompanied by PanIN lesions and 7 patients with other types of pancreatic tumors (neuroendocrine tumor, 2; serous cystic neoplasm, 2; solid pseudopapillary neoplasm, 1; epithelial cyst, 1; and hamartoma, 1) who underwent pancreas resection without preoperative therapy between March 2009 and March 2012. The use of resected samples was approved by the Institutional Review Board for Clinical Research at Osaka University Hospital (14435). Written informed consent was obtained from each patient. These samples were sectioned (4 μm) and stained with H&E. The sections also were

stained for Bcl-xL immunohistochemistry. The slides were treated by immersion in 1× Target Retrieval Solution (pH 6.0) (Dako) and heated to 120°C in a decloaking chamber. They were incubated with 3% hydrogen peroxide in methanol for 15 minutes to quench the endogenous peroxidase activity. After blocking with 5% goat serum for 1 hour, they were incubated with anti–Bcl-xL antibody (1:200, 2764; Cell Signaling Technology) overnight at 4°C. After the incubation with secondary antibody (SignalStain Boost IHC detection reagent; Cell Signaling Technology) for 30 minutes, the sections were developed with 3,3'-diaminobenzidine for 2 minutes and counterstained with hematoxylin. Negative controls were performed by omitting the primary antibody. The total score for each sample was the average score obtained from 6 high-power (magnification, ×200) microscopic fields.

Cell Lines and Culture Conditions

The human pancreatic cancer cell lines PANC-1 and MIA PaCa-2 were purchased from the American Type Culture Collection (Manassas, VA). These cells were cultured in Dulbecco's modified Eagle medium containing 10% heat-inactivated fetal bovine serum and antibiotic–antimycotic (Thermo Fisher Scientific, Rockford, IL) in a 5% CO_2 atmosphere at 37°C. PANC-1 and MIA PaCa-2 cells were transfected with Bcl-xL small interfering RNAs (siRNAs) (s1920-22; Thermo Fisher Scientific) using Lipofectamine RNAiMAX Transfection Reagent (Thermo Fisher Scientific) according to the manufacturer's protocol.

Apoptosis Assay and Cell Viability

Cells were assayed for apoptosis by monitoring caspase-3/7 activity using the Caspase-Glo assay (Promega, Madison, WI) according to a previously described procedure.[25] Cell viability was evaluated by the water-soluble tetrazolium salt (WST) assay with cell count reagent SF (Nacalai Tesque, Kyoto, Japan).

Western Blot Analysis

The Western blot analysis was performed using a previously described method.[26] The following antibodies were used: anti–Bcl-xL antibody, anti–Bcl-2 antibody, anti–Mcl-1 antibody (Cell Signaling Technology), anti-p21 antibody (Santa Cruz Biotechnology), and anti–β-actin antibody (Sigma-Aldrich, St. Louis, MO).

Statistical Analysis

Survival curves were plotted using the Kaplan–Meier method and compared by the log-rank test using Statistics Package for Social Science software version 21.0 (SPSS, Inc, Chicago, IL). The data were presented as the means ± SD or medians and interquartile range, with comparisons using the Student *t* test or the Mann–Whitney *U* test, respectively. The incidences of PDAC were compared using the Fisher exact test. *P* values less than .05 were considered statistically significant.

All authors had access to the study data and reviewed and approved the final manuscript.

Results

Bcl-xL Expression Increases in Both PanINs and PDAC

To analyze Bcl-xL expression levels in PanINs and PDAC, pancreas sections were examined in pancreas-specific Kras-mutated mice (*Pdx1-Cre LSL-KrasG12D* mice [P-KrasG12D mice]). Control littermates of *Pdx1-Cre* mice did not show any histologic changes in the pancreas from 2 to 14 months (Figure 1*A* and *B*). In contrast, P-KrasG12D mice showed sporadic PanIN-1 lesions at 2 months. The number of PanINs and their grade gradually progressed at 4 months and increased further at 7 months (Figure 1*A* and *C*). At 12–14 months, widespread low- to high-grade PanINs were detected in all mice, and invasive ductal adenocarcinomas developed in 5 of 9 mice (55.6%) (Figure 1*A*). The percentage of normal-appearing areas in pancreas sections significantly decreased with age (Figure 1*B*). Immunohistochemistry showed Bcl-xL overexpression in the cytoplasm of PDACs from P-KrasG12D mice, consistent with previous reports of resected specimens from human beings[13,14] (Figure 1*D* and *E*). Of importance, Bcl-xL was overexpressed significantly, even in PanIN-1. Bcl-xL overexpression was augmented in PanIN-2/3 and enhanced further in PDAC (Figure 1*D* and *E*). As shown in Western blot analysis, Bcl-xL expression levels were increased in the pancreas of P-KrasG12D mice compared with those in control littermates at 4 months, and gradually increased with age (Figure 1*F*). We also examined other anti-apoptotic Bcl-2 family proteins, including Mcl-1 and Bcl-2.[27] Mcl-1 expression levels were increased slightly in P-KrasG12D mice, whereas Bcl-2 expression levels did not increase (Figure 1*F*).

Next, we evaluated Bcl-xL expression levels in PanINs using clinical resected samples. Consistent with the murine results, Bcl-xL also was overexpressed in the cytoplasm of human PanINs and PDAC samples (Figure 2). Total immunostaining scores were increased significantly in human PanIN-1 compared with those in normal human pancreatic ducts, and were increased further with the progression to human PanIN-2/3 and human PDAC (Figure 2). Collectively, Bcl-xL was overexpressed in early stage PanINs and increased with the progression of pancreatic neoplasia.

Bcl-xL Overexpression in Kras-Mutated Cells Promotes PDAC Carcinogenesis

Next, we examined the impact of Bcl-xL overexpression on the development of PanINs and PDAC. For this purpose, we generated Bcl-xL Tg P-KrasG12D mice by mating P-KrasG12D mice and Bcl-xL Tg mice. We confirmed that Bcl-xL expression levels in the pancreas were increased remarkably in Bcl-xL Tg mice compared with those in control wild-type littermates (Figure 3*A*). In physiological settings, Bcl-xL Tg mice did not show histologic abnormalities of the pancreas (Figure 3*B*) or any significant differences in pancreas/body weight ratios or serum levels of

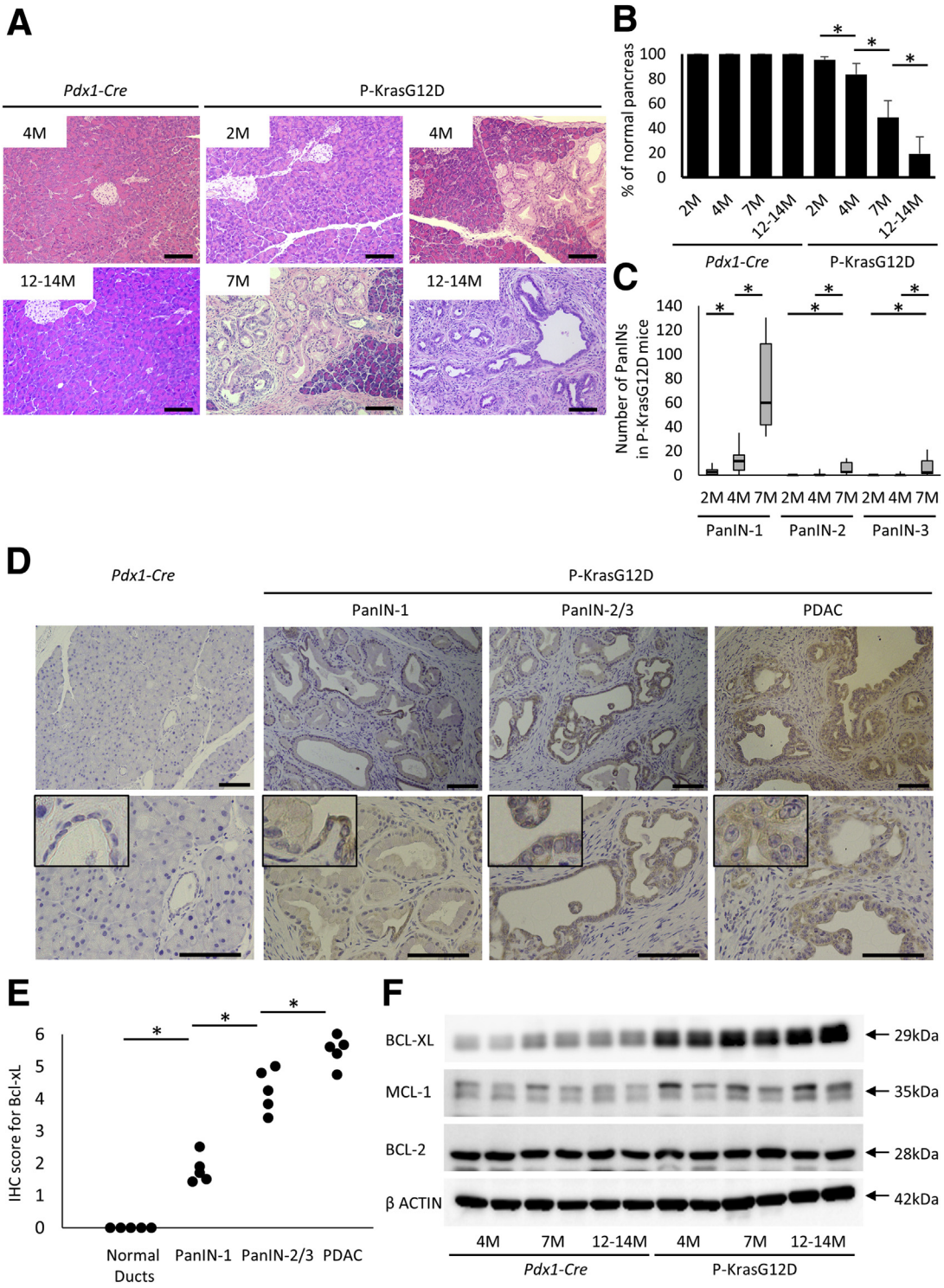

Figure 1. Bcl-xL expression levels are enhanced gradually from PanIN-1 to PDAC in P-KrasG12D mice. (*A–C*) P-KrasG12D mice (*Pdx1-Cre; LSL-KrasG12D*) (n = 12 at 2 mo, 10 at 4 mo, 6 at 7 mo, and 9 at 12–14 mo) or wild-type littermates (*Pdx1-Cre*) (n = 10 at 2 mo, 6 at 4 mo, 4 at 7 mo, and 10 at 12–14 mo) were killed at the indicated months. (*A*) Representative pictures of H&E staining. *Scale bar*: 100 μm (original magnification, ×200). (*B*) The percentage of normal pancreas in defined area. *$P < .05$. (*C*) The number of PanINs per defined area in the pancreas sections of P-KrasG12D mice. (*D*) Representative images of Bcl-xL immunohistochemical staining of pancreas sections in wild-type mice and P-KrasG12D mice at 12–14 months. *Scale bar*: 100 μm (original magnification, ×200 in the upper row and ×400 in the lower row; width of insets: 50 μm). (*E*) Total score for the immunostaining of Bcl-xL in normal pancreatic ducts from wild-type mice (n = 5) and PanINs/PDAC from P-KrasG12D mice at 12–14 months (n = 5). (*F*) Western blot of anti-apoptotic Bcl-2 family proteins in the pancreas of P-KrasG12D mice.

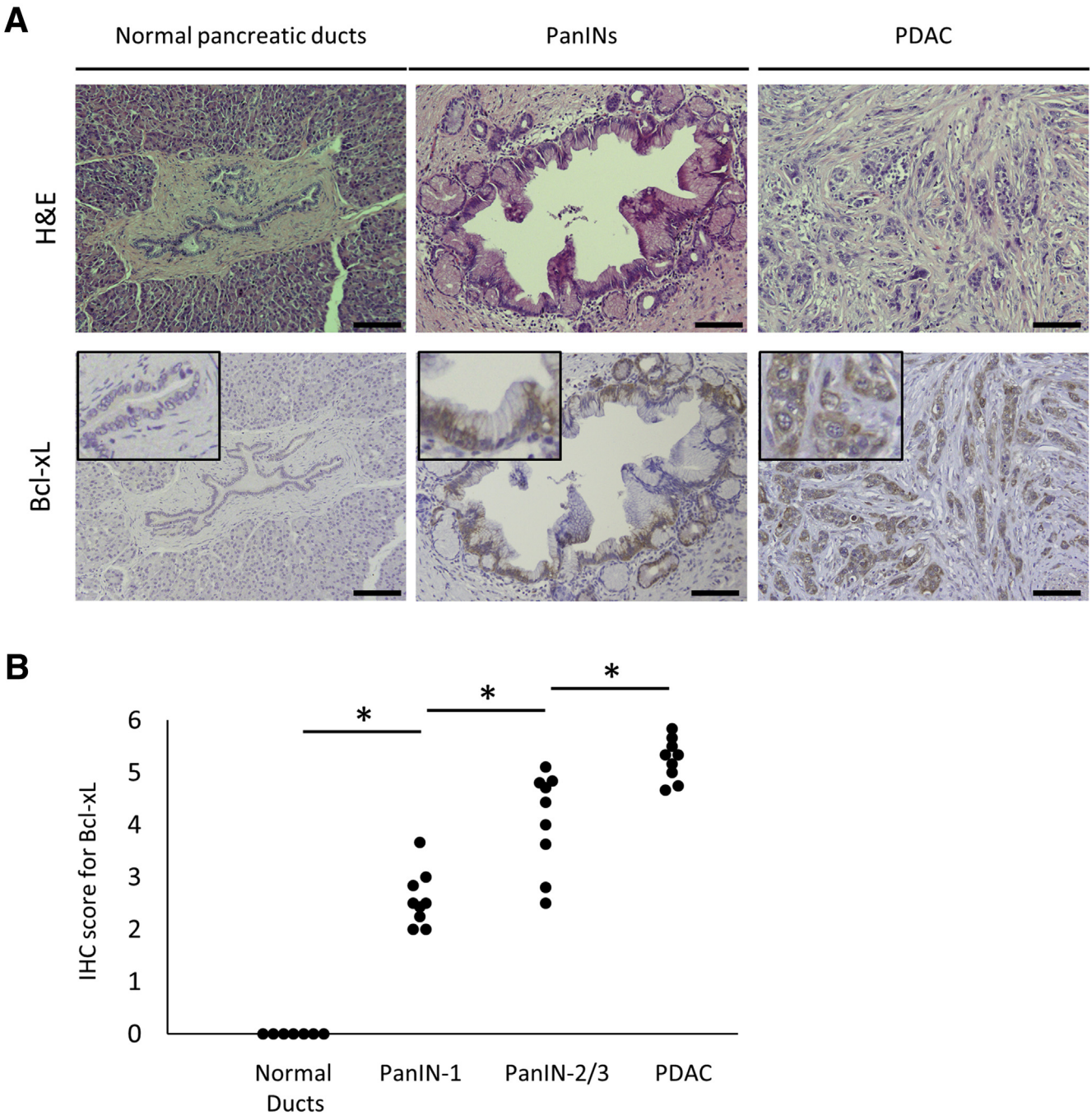

Figure 2. Bcl-xL expression levels are increased in human PanINs and PDAC. Human resected pancreatic tissues of 9 patients with PDAC accompanied by PanIN lesions and 7 patients with other types of pancreatic tumors were stained with H&E and anti–Bcl-xL antibody. Given that the pancreatic tissues of 9 patients with PDAC contained many PanINs in the nontumor area, normal pancreatic ducts were evaluated using nontumor areas of pancreatic tissues from 7 patients with other types of pancreatic tumors. (*A*) Representative images of H&E and Bcl-xL immunohistochemistry staining of pancreas sections. *Scale bar*: 100 μm (original magnification, $\times$200); width of insets: 100 μm. (*B*) Total score for the immunostaining of Bcl-xL. *$P < .05$.

amylase and lipase compared with littermate wild-type mice (Figure 3*C*). To examine the impact of Bcl-xL overexpression on carcinogenesis, we compared Bcl-xL Tg P-KrasG12D mice with their P-KrasG12D littermates. Up-regulation of Bcl-xL in the pancreas of Bcl-xL Tg P-KrasG12D mice compared with P-KrasG12D mice was confirmed by Western blot analysis (Figure 4*A*). Stronger Bcl-xL expression was observed in the cytoplasm of PanINs and PDAC from Bcl-xL Tg P-KrasG12D mice than in that from P-KrasG12D mice, as assessed by immunohistochemistry (Figure 4*B*). P-KrasG12D mice had no macroscopic or microscopic PDAC at 2, 4, or 7 months (Figure 4*C*–*E*). In contrast, 41.7% (5 of

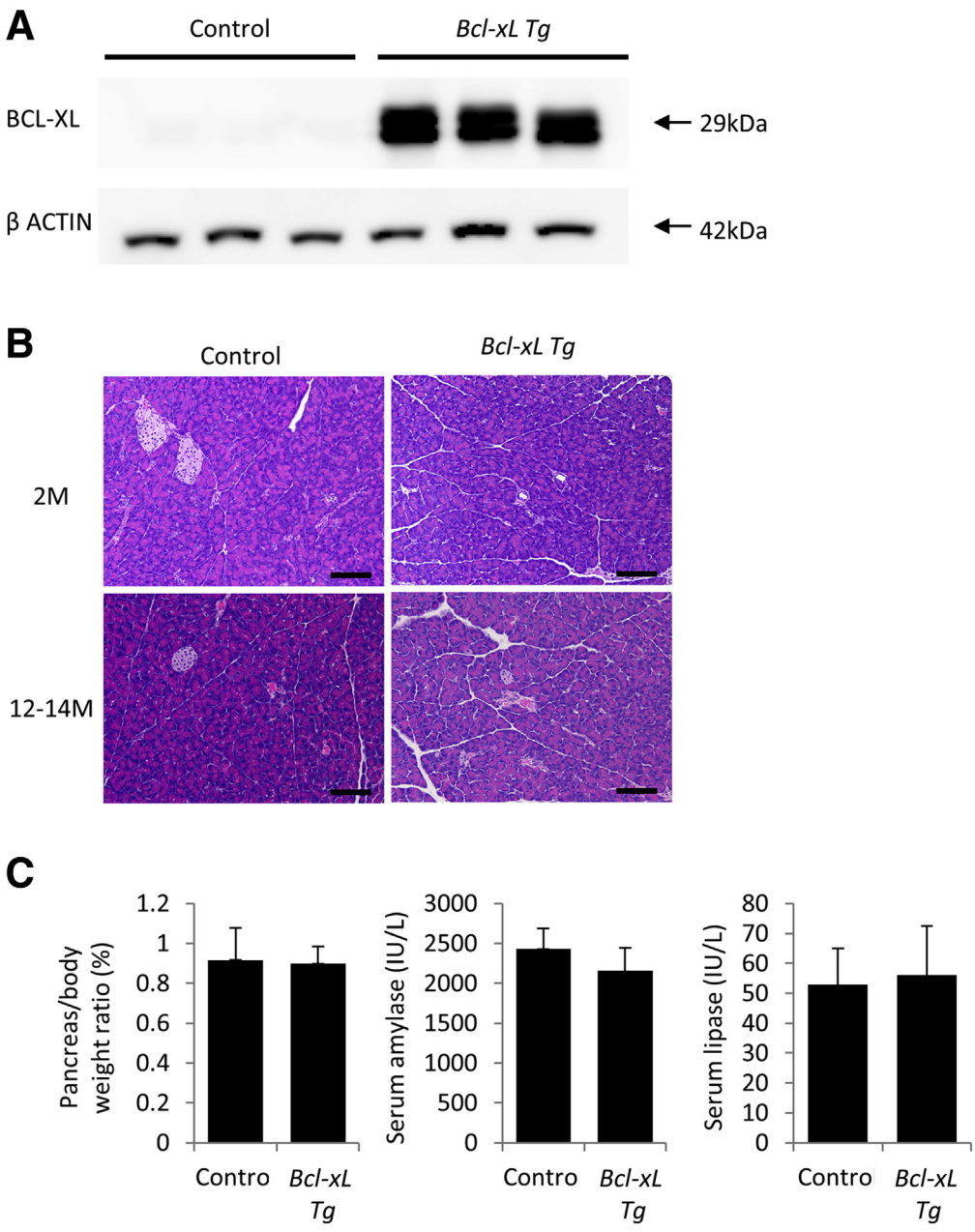

Figure 3. Bcl-xL–overexpressing mice do not show any phenotype under physiological conditions. Bcl-xL Tg mice and their control littermates were killed at 2 and 12 months. (*A*) Western blot analysis of Bcl-xL in the pancreas at 2 months. (*B*) Representative images of H&E staining of pancreas sections at 2 and 12–14 months. *Scale bar*: 100 μm (original magnification, $\times$200). (*C*) Pancreas/body weight ratio and serum levels of amylase and lipase at 2 months (n = 5 in Bcl-xL Tg mice, n = 4 in control mice).

12) of Bcl-xL Tg P-KrasG12D mice developed microscopic PDAC at 2 months, and 8.3% (1 of 12) developed macroscopically visible PDAC (Figure 4*D* and *E*). At 4 and 7 months, all had developed macroscopically evident PDAC (Figure 4*C*–*E*). H&E staining showed that the area of the normal-appearing pancreas of Bcl-xL Tg P-KrasG12D mice was significantly smaller than that of P-KrasG12D mice (Figure 4*F*), and the number of PanIN-2/3 lesions in the pancreas of Bcl-xL Tg P-KrasG12D mice at 2 months was significantly larger than that of P-KrasG12D mice at 2 months (Figure 4*G*). All Bcl-xL Tg P-KrasG12D mice died within 1 year; their median survival was 7.8 months (Figure 4*H*), which was significantly shorter than their P-KrasG12D littermates. These data suggest that Bcl-xL overexpression accelerates carcinogenesis of Kras-mutated pancreatic neoplasia, reducing survival in P-KrasG12D mice.

Bcl-xL Overexpression Suppresses Oncogene-Induced Senescence in Low-Grade PanINs and Apoptosis in High-Grade PanINs

To address the mechanisms by which Bcl-xL overexpression promotes PDAC carcinogenesis, we examined the effect of apoptosis in PanIN lesions and PDAC. We compared P-KrasG12D mice at 12–14 months with Bcl-xL Tg P-KrasG12D mice at 2 months because both had low-grade PanINs as well as high-grade PanINs and PDAC. The percentage of TUNEL-positive cells was 0.44% ± 0.19% in

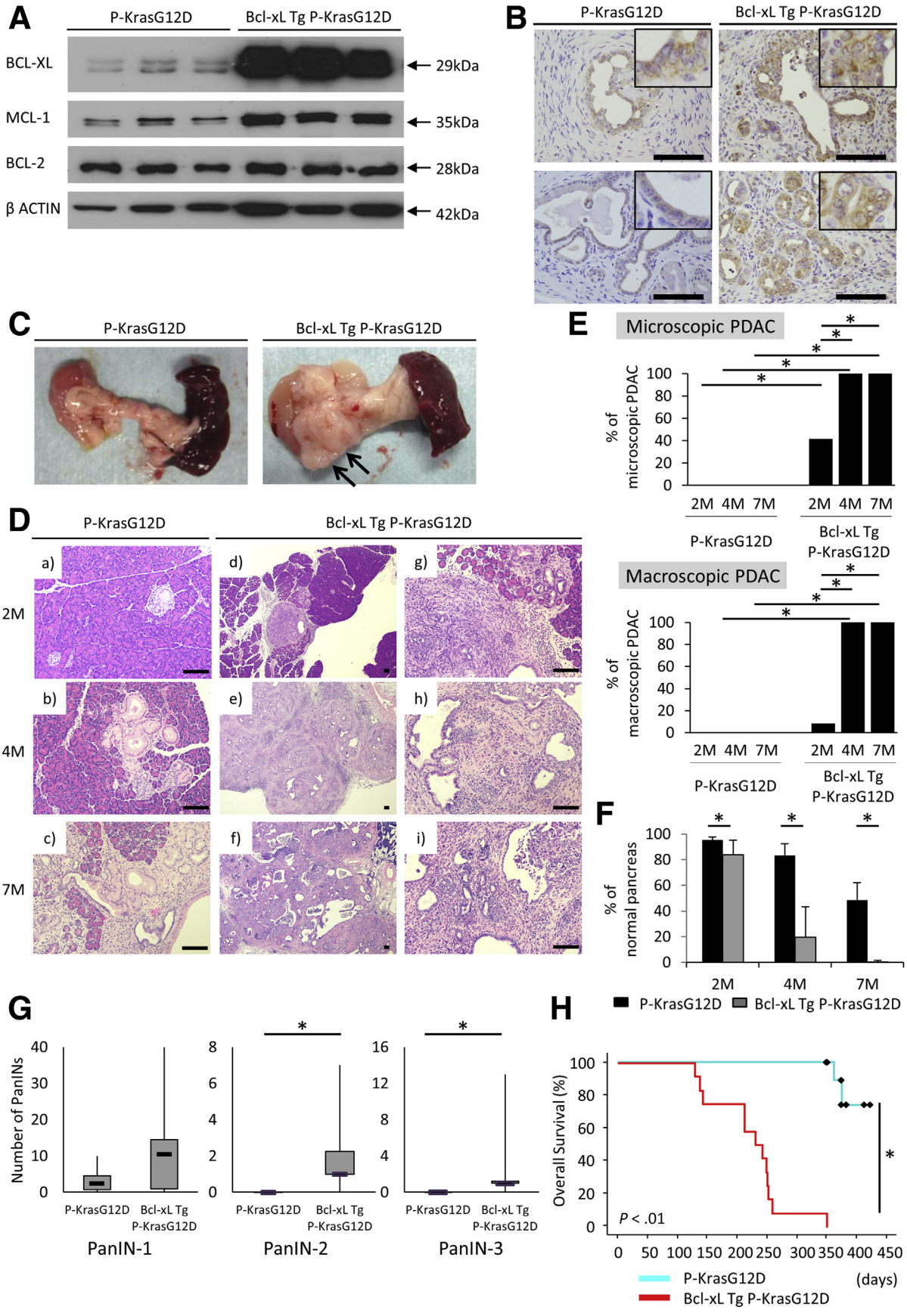
A
P-KrasG12D
Bcl-xL Tg P-KrasG12D
BCL-XL
MCL-1
BCL-2
β ACTIN
29kDa
35kDa
28kDa
42kDa
B
P-KrasG12D
Bcl-xL Tg P-KrasG12D
C
P-KrasG12D
Bcl-xL Tg P-KrasG12D
D
P-KrasG12D
Bcl-xL Tg P-KrasG12D
2M
4M
7M
a)
b)
c)
d)
e)
f)
g)
h)
i)
E
Microscopic PDAC
% of microscopic PDAC
2M 4M 7M 2M 4M 7M
P-KrasG12D
Bcl-xL Tg P-KrasG12D
Macroscopic PDAC
% of macroscopic PDAC
F
% of normal pancreas
2M
4M
7M
P-KrasG12D
Bcl-xL Tg P-KrasG12D
G
Number of PanINs
P-KrasG12D
Bcl-xL Tg P-KrasG12D
PanIN-1
PanIN-2
PanIN-3
H
Overall Survival (%)
P < .01
(days)
P-KrasG12D
Bcl-xL Tg P-KrasG12D

PanIN-1, 0.66% ± 0.69% in PanIN-2, and 1.21% ± 0.50% in PanIN-3 of P-KrasG12D mice (Figure 5*A* and *B*). The frequency of TUNEL-positive cells in PanIN-1 and PanIN-2 did not decrease significantly with Bcl-xL overexpression, whereas the number of TUNEL-positive cells decreased significantly in PanIN-3 (Figure 5*A* and *B*). These data suggest that Bcl-xL overexpression might not have an effect on apoptosis in low-grade PanIN lesions. In contrast, Bcl-xL overexpression suppressed apoptosis in high-grade PanIN-3.

Next, we further examined another mechanism of acceleration of carcinogenesis in Bcl-xL Tg P-KrasG12D mice. We examined senescence in P-KrasG12D mice and Bcl-xL Tg P-KrasG12D mice using SA–β-gal activity, which is a specific detector of senescence.[28] In 12- to 14-month P-KrasG12D mice, SA–β-gal–positive cells were observed frequently in PanIN-1, but were decreased remarkably in PanIN-2/3 and PDAC (Figure 5*C*). In contrast, few positive cells were detected in the PanIN-1, PanIN-2/3, and PDAC lesions from Bcl-xL Tg P-KrasG12D mice at 2 months (Figure 5*C*). Immunostaining for p21, another marker associated with oncogene-induced senescence,[29] also showed that the number of p21-positive cells in PanIN-1 lesions was reduced significantly in Bcl-xL Tg P-KrasG12D mice at 2 months compared with that in P-KrasG12D mice at 12–14 months (Figure 5*D* and 5*E*). There were few p21-positive PanIN-2/3 and PDAC cells in both mice (Figure 5*D* and *E*). These data suggest that oncogene-induced senescence is induced in PanIN-1 of P-KrasG12D mice and that it is inhibited by the increase in Bcl-xL expression levels.

Bcl-xL Deficiency in Kras-Mutated Cells Increases the Number of Senescent Cells in High-Grade PanINs

Next, we examined the impact of Bcl-xL deficiency on the induction of senescence in PanINs. Pancreas-specific Bcl-xL knockout mice without the Kras mutation (*bcl-x*$^{flox/flox}$ *Pdx1-Cre* mice) did not show any phenotype under physiological conditions (Figure 6). We generated pancreas-specific Kras-mutated and Bcl-xL knockout mice (Bcl-xL knockout [KO] P-KrasG12D mice) by mating P-KrasG12D mice and *bcl-x*$^{flox/flox}$ mice (Figure 7*A* and *B*). SA–β-gal–positive cells were observed frequently in PanIN-1 lesions from both Bcl-xL KO P-KrasG12D mice and P-KrasG12D mice. Positive cells also were detected in PanIN-2/3 lesions from Bcl-xL KO P-KrasG12D mice, but rarely were observed in PanIN-2/3 lesions from P-KrasG12D mice (Figure 7*C*). According to the immunostaining for p21, the percentage of p21-positive cells in PanIN-2/3 lesions was significantly higher in Bcl-xL KO P-KrasG12D mice than in P-KrasG12D mice, but a significant difference was not detected in the PanIN-1 lesions from these mice (Figure 7*D* and *E*). The frequency of TUNEL-positive cells in PanIN lesions of any grade did not increase significantly with Bcl-xL deficiency in P-KrasG12D mice (Figure 7*F* and *G*). A lower percentage of Bcl-xL KO P-KrasG12D mice developed PDAC at 12 months than littermate P-KrasG12D mice (35.7% [5 of 14] vs 83.3% [5 of 6]), although the difference did not reach statistical significance ($P = .07$). These results suggest that Bcl-xL inhibition increases the number of senescent cells in high-grade PanINs, which might suppress the progression from PanINs to PDAC.

Bcl-xL Inhibition Induces Oncogene-Induced Senescence and Apoptosis in PDAC

Finally, to examine the possibility of apoptotic induction and oncogene-induced senescence by Bcl-xL inhibition in PDAC, PANC-1 and MIA PaCa-2 cells were treated with siRNAs against Bcl-xL. siRNA-mediated knockdown of Bcl-xL led to a significant increase in caspase-3/7 activity and a significant decrease in cell viability (Figure 8*A*). Bcl-xL knockdown increased p21 expression levels, as evaluated by Western blot analysis (Figure 8*B*). Bcl-xL knockdown also significantly increased the number of β-galactosidase–positive cells (Figure 8*C*). Collectively, these data suggest that Bcl-xL inhibition efficiently induces oncogene-induced senescence and apoptosis in PDAC.

Discussion

Bcl-xL overexpression has been observed in several types of cancer[30,31] and is associated with tumor growth, malignant biological behaviors, and survival.[32–34] According to previous studies of PDAC, Bcl-xL up-regulation is observed frequently in human samples[13,14,35] and is associated with a poorer prognosis,[23] but the effect of Bcl-xL overexpression during PDAC carcinogenesis and whether Bcl-xL expression is observed in precancerous PanIN lesions has not been investigated completely. As shown in this study, Bcl-xL expression was increased significantly in the cytoplasm of PanIN-1 lesions compared with that in normal pancreatic ducts, and was augmented gradually with the progression of pancreatic neoplasia in Kras mutant mouse models and human samples (Figures 1*D–F* and 2*A* and *B*). We report that Bcl-xL expression increases in PanINs as well as PDAC.

Figure 4. (***See previous page***). **Bcl-xL overexpression accelerates the incidence rate of PDAC and reduces survival time in P-KrasG12D mice.** P-KrasG12D mice and Bcl-xL Tg P-KrasG12D mice were killed at the indicated months. (*A*) Western blot of anti-apoptotic Bcl-2 family proteins in the pancreas at 4 months. (*B*) Representative images of pancreas sections at 4 months stained for Bcl-xL. *Scale bar*: 100 μm (original magnification, ×400); width of insets: 50 μm. (*C*) Macroscopic pictures of the pancreas at 4 months. *Arrows*, macroscopically evident tumors. (*D*) Representative images of H&E staining of pancreas sections. *Scale bar*: 100 μm (original magnification for *A–F*, ×40; *G–I*, ×200). (*E*) The ratio of microscopic and macroscopic PDAC $^*P < .05$. (*F*) The percentage of normal pancreas at 2 months (n = 12 per each), 4 months (n = 10 or 11), and 7 months (n = 6 per each). $^*P < .05$. (*G*) The number of PanINs per defined area in the pancreas sections of P-KrasG12D mice and Bcl-xL Tg P-KrasG12D mice (n = 12 per group) at 2 months $^*P < .05$. (*H*) Kaplan–Meier survival analysis of P-KrasG12D (n = 11) and Bcl-xL Tg P-KrasG12D mice (n = 12). $^*P < .05$.

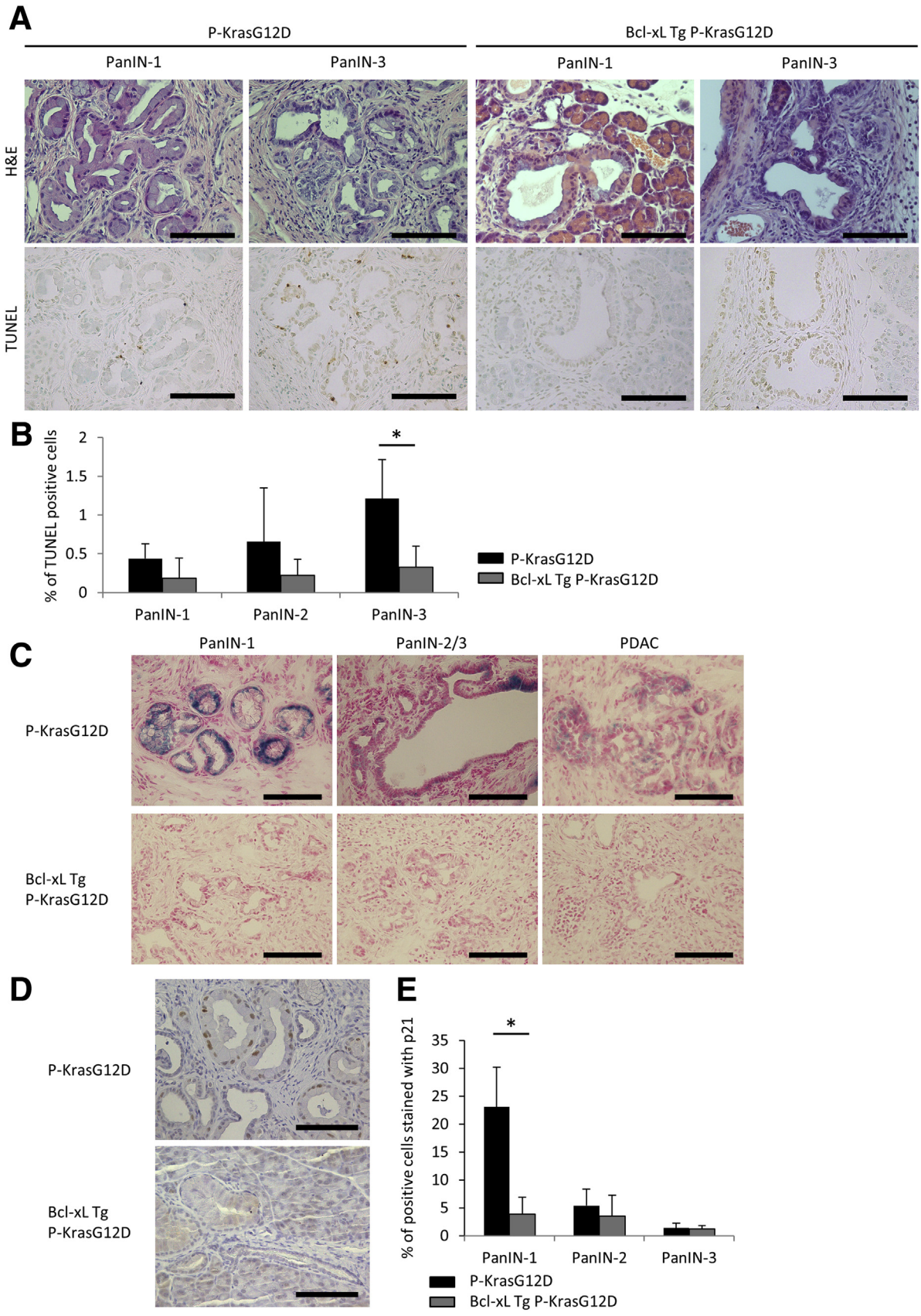
A
P-KrasG12D
Bcl-xL Tg P-KrasG12D
PanIN-1
PanIN-3
PanIN-1
PanIN-3
H&E
TUNEL
B
% of TUNEL positive cells
2
1.5
1
0.5
0
*
PanIN-1
PanIN-2
PanIN-3
P-KrasG12D
Bcl-xL Tg P-KrasG12D
C
PanIN-1
PanIN-2/3
PDAC
P-KrasG12D
Bcl-xL Tg
P-KrasG12D
D
P-KrasG12D
Bcl-xL Tg
P-KrasG12D
E
% of positive cells stained with p21
35
30
25
20
15
10
5
0
*
PanIN-1
PanIN-2
PanIN-3
P-KrasG12D
Bcl-xL Tg P-KrasG12D

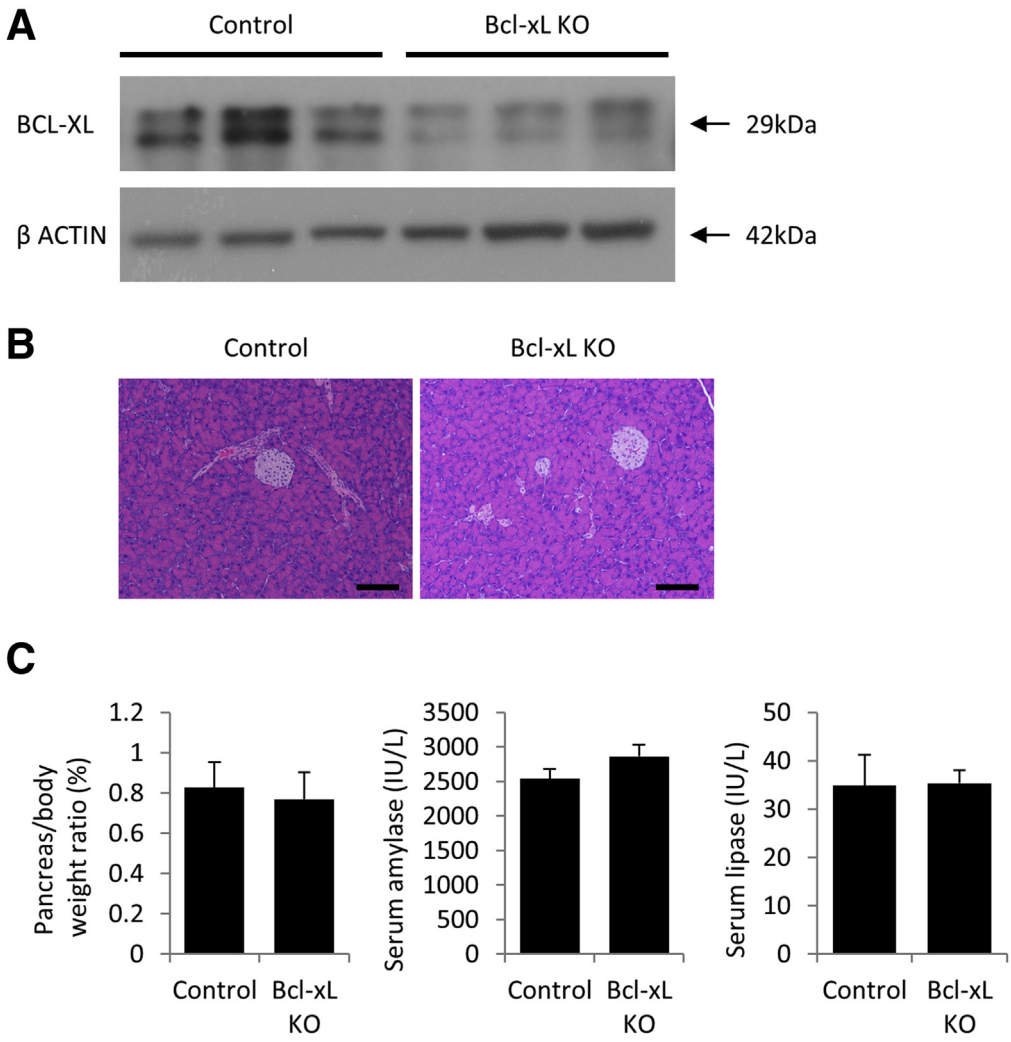

Figure 6. Pancreas-specific Bcl-xL–knockout mice do not show any phenotype under physiological conditions. Bcl-xL KO mice (*bcl-x*$^{flox/flox}$ *Pdx1-Cre*) and their control littermates (*bcl-x*$^{flox/flox}$) were killed at the indicated months. (*A*) Western blot analysis of Bcl-xL in the pancreas at 2 months. (*B*) Representative images of H&E staining of pancreas sections at 6 months. *Scale bar*: 100 μm (original magnification, $\times$200). (*C*) Pancreas/body weight ratio and serum amylase and lipase levels at 6 months (n = 11 in Bcl-xL KO mice and n = 7 in control mice).

As clearly shown in the present study, Bcl-xL overexpression led to the acceleration of carcinogenesis in Kras-mutated pancreatic neoplasia. All Bcl-xL Tg P-KrasG12D mice developed grossly evident PDAC at as early as 4 months, whereas P-KrasG12D mice showed only microscopic PanIN lesions (Figure 4*C*–*E*). Genetically engineered mouse models of PDAC are based commonly on Kras mutations,[9] and various mutations or deletions of genes, such as p53,[36] Ink4a,[15] and transforming growth factor-β,[37] result in rapid carcinogenesis of Kras-mutated pancreatic neoplasia. However, no murine PDAC models have been reported to harbor gene mutations or deletions in Bcl-2 family proteins. This study showed accelerated pancreatic carcinogenesis using a mouse model of Bcl-2 family proteins. The results showing that 41.7% (5 of 12) of Bcl-xL Tg P-KrasG12D mice developed microscopic PDAC at as early as 2 months (Figure 4*D* and *E*) and the number of microscopic PanIN-2/3 lesions was increased significantly compared with that in P-KrasG12D mice (Figure 4*G*) suggest that Bcl-xL up-regulation in the presence of Kras mutation causes the rapid progression of low-grade PanINs to high-grade PanINs and PDAC, reducing the survival of Bcl-xL Tg P-KrasG12D mice (Figure 4*H*). The overexpression of anti-apoptotic proteins, including Bcl-xL, in tumor cells directly accelerates tumor proliferation by inhibiting apoptosis.[32,38] Together with the in vitro findings that

Figure 5. (*See previous page*). Bcl-xL overexpression suppresses oncogene-induced senescence in low-grade PanINs and apoptosis in high-grade PanINs. (*A* and *B*) Pancreatic tissues of P-KrasG12D mice at 12–14 months and Bcl-xL Tg P-KrasG12D mice at 2 months were stained with H&E and TUNEL (n = 5 per group). (*A*) Representative images of H&E and TUNEL staining and (*B*) the percentage of TUNEL-positive cells. *Scale bar*: 100 μm (original magnification, $\times$400). (*C*–*E*) Pancreatic tissues of P-KrasG12D mice at 12–14 months and Bcl-xL Tg P-KrasG12D mice at 2 months were stained for SA–β-gal activity and stained with anti-p21 antibody (n = 5 per group). (*C*) Representative images of staining for SA–β-gal activity. Scale bar: 100 μm (original magnification, $\times$400). (*D*) Representative images of p21 staining of pancreas sections and (*E*) the percentage of p21-positive cells. *Scale bar*: 100 μm (original magnification, $\times$400). *$P < .05$.

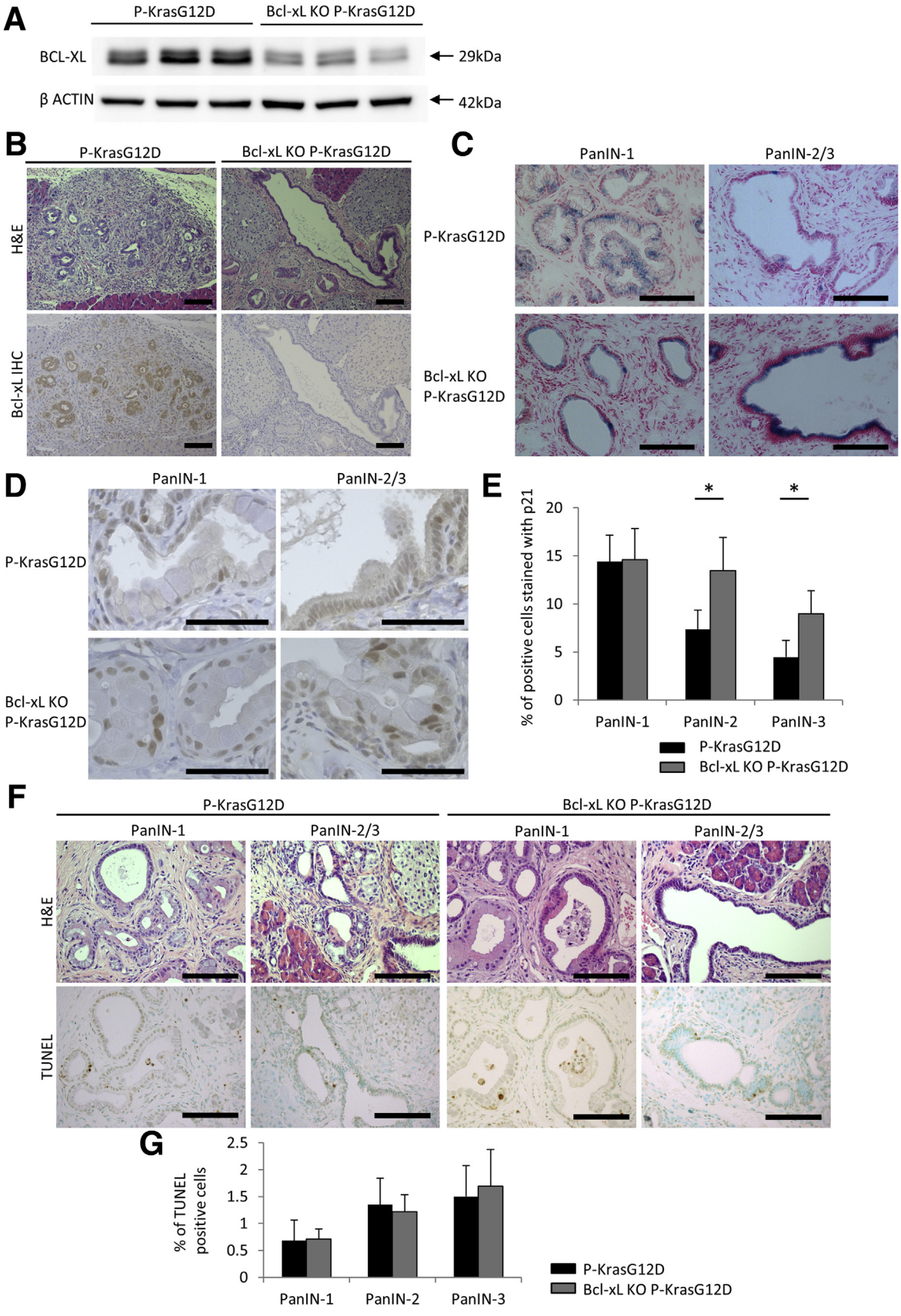
A
P-KrasG12D
Bcl-xL KO P-KrasG12D
BCL-XL
29kDa
β ACTIN
42kDa
B
P-KrasG12D
Bcl-xL KO P-KrasG12D
H&E
Bcl-xL IHC
C
PanIN-1
PanIN-2/3
P-KrasG12D
Bcl-xL KO
P-KrasG12D
D
PanIN-1
PanIN-2/3
P-KrasG12D
Bcl-xL KO
P-KrasG12D
E
% of positive cells stained with p21
20
15
10
5
0
*
*
PanIN-1
PanIN-2
PanIN-3
P-KrasG12D
Bcl-xL KO P-KrasG12D
F
P-KrasG12D
Bcl-xL KO P-KrasG12D
PanIN-1
PanIN-2/3
PanIN-1
PanIN-2/3
H&E
TUNEL
G
% of TUNEL positive cells
2.5
2
1.5
1
0.5
0
PanIN-1
PanIN-2
PanIN-3
P-KrasG12D
Bcl-xL KO P-KrasG12D

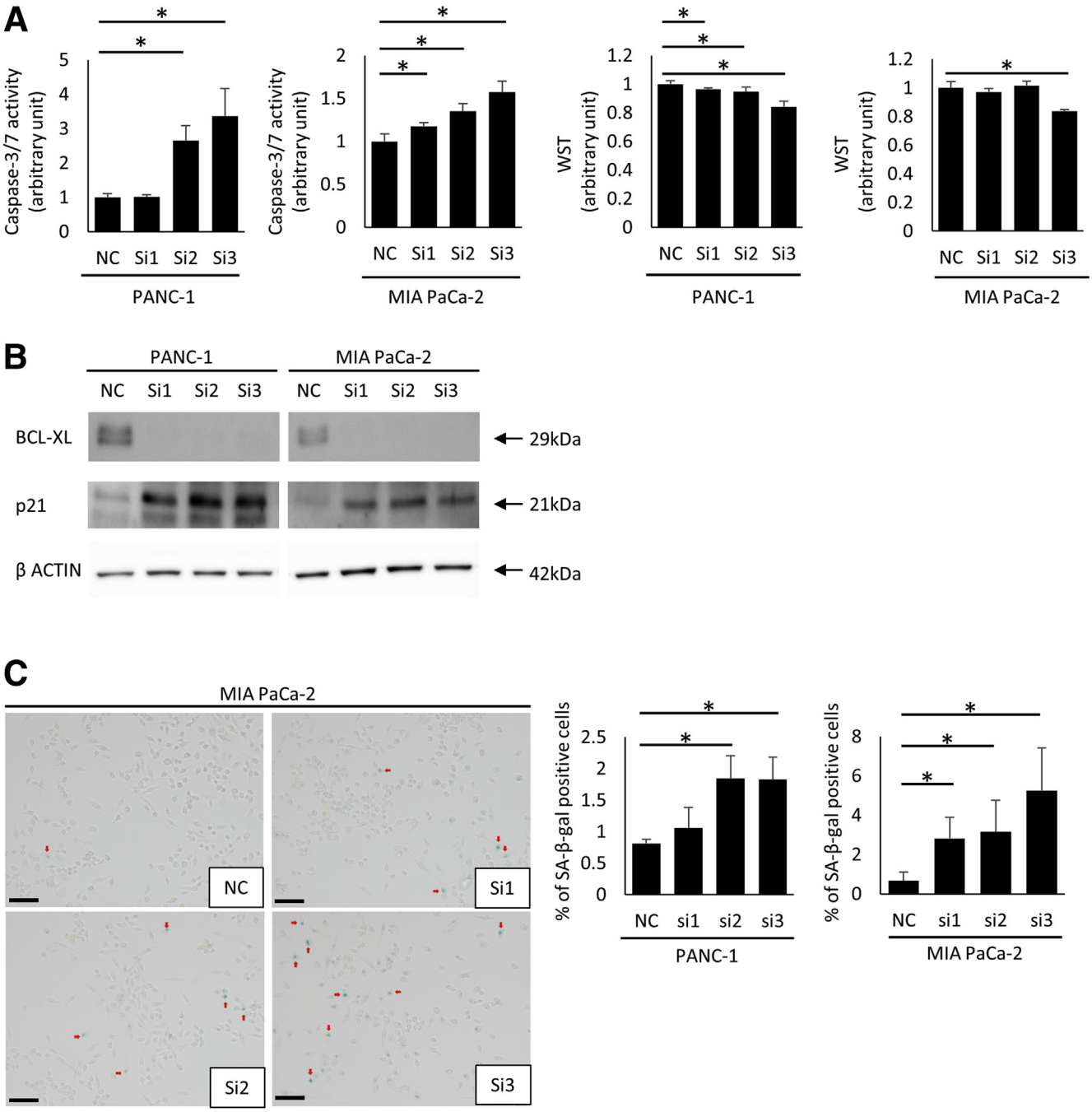

Figure 8. Oncogene-induced senescence is induced by Bcl-xL inhibition in vitro. PANC-1 and MIA Paca-2 cells were transfected with Bcl-xL siRNAs (si1, si2, si3) or negative control siRNA (NC) for 24 hours. After changing the medium, cells were incubated for an additional 24 hours (caspase-3/7 activity) and for 48 hours (WST assay, Western blot analysis, and SA–β-gal activity). (*A*) Caspase-3/7 activity in culture supernatants and cell viability was determined by the WST assay (n = 4). (*B*) Western blot of Bcl-xL and p21. (*C*) Representative images of PDAC cells stained for SA–β-gal activity and the percentage of SA–β-gal–positive cells. *Scale bar*: 100 μm. *$P < .05$.

Figure 7. (***See previous page***). **Bcl-xL deficiency increases senescence in high-grade PanINs.** Bcl-xL KO P-KrasG12D mice (*bcl-x$^{flox/flox}$ Pdx1-Cre LSL-KrasG12D*) (n = 14) and their littermate P-KrasG12D mice (*bcl-x$^{+/+}$ Pdx1-Cre LSL-KrasG12D*) (n = 6) were killed at 12 months. (*A*) Western blot of Bcl-xL in the pancreas. (*B*) Representative images of pancreas sections stained for Bcl-xL. *Scale bar*: 100 μm (original magnification, $\times$200). (*C*) Representative images of staining for SA–β-gal activity. *Scale bar*: 100 μm (original magnification, $\times$400). (*D*) Representative images of p21 staining in pancreas sections and (*E*) the percentage of p21-positive cells. *Scale bar*: 50 μm (original magnification, $\times$1200). *$P < .05$. (*F*) Representative images of H&E and TUNEL staining and (*G*) the percentage of TUNEL-positive cells. *Scale bar*: 100 μm (original magnification, $\times$400).

siRNA-mediated Bcl-xL knockdown in Kras-mutated PDAC cells decreased cell viability and increased apoptosis (Figure 8*A*), accelerated tumor cell proliferation caused by Bcl-xL overexpression, also may contribute to the reduced survival. Bcl-xL staining recently was detected in the nucleus and cytoplasm of PDAC.[35] As reported by Choi et al,[39] nuclear Bcl-xL promotes the epithelial–mesenchymal transition, migration, invasion, and stemness of cell lines derived from pancreatic neuroendocrine tumors and breast cancer. In the present study, we observed Bcl-xL immunostaining in the cytoplasm of PanINs and PDAC, consistent with previous immunohistochemical studies of PDAC,[23,40] but we did not detect immunopositivity in the nucleus (Figures 1*D*, 2*A*, and 4*B*). However, there remains a possibility that nuclear Bcl-xL, which may be expressed in undetectable levels by immunohistochemistry, affects the development of PDAC in Bcl-xL Tg P-KrasG12D mice.

In the present study, we addressed 2 possible mechanisms by which Bcl-xL overexpression accelerated the progression to high-grade PanINs and PDAC in Kras mutant mice: inhibition of apoptosis and inhibition of oncogene-induced senescence. Bcl-xL is an anti-apoptotic protein,[27] and its overexpression is expected to inhibit PanIN apoptosis, resulting in the acceleration of carcinogenesis. A small number of apoptotic cells was observed in PanIN-1 lesions from P-KrasG12D mice (Figure 5*A* and *B*), consistent with a previous report of resected samples from human beings.[41] Bcl-xL overexpression in Kras-mutated neoplasia did not significantly decrease the number of apoptotic cells in PanIN-1 lesions (Figure 5*A* and *B*). In contrast, the number of apoptotic cells was suppressed significantly by Bcl-xL overexpression in PanIN-3 (Figure 5*A* and 5*B*). Kras mutation induces oncogene-induced senescence,[42] which is regarded as a tumor-suppressive effect because the suppression of senescence leads to the rapid progression to high-grade PanINs and PDAC.[43,44] In the present study, oncogene-induced senescent cells were observed frequently in PanIN-1 lesions from P-KrasG12D mice, but not in PanIN-2/3 and PDAC lesions (Figure 5*C*–*E*). Importantly, Bcl-xL overexpression strongly suppressed the oncogene-induced senescence observed in the PanIN-1 lesions from P-KrasG12D mice (Figure 5*C*–*E*). These data suggest that the suppressive effect of Bcl-xL overexpression on oncogene-induced senescence shows a greater impact on low-grade PanINs than high-grade PanINs. As shown by Yosef et al,[45] joint inhibition of Bcl-w and Bcl-xL, but not single inhibition of Bcl-xL, eliminates senescent fibroblasts by inducing apoptosis. In the present study, Bcl-xL overexpression decreased the number of senescent cells in PanIN-1 lesions from P-KrasG12D mice without inducing apoptosis (Figure 5). Although Yosef et al[45] described the effect of Bcl-xL on apoptosis in senescent cells, we reported the effect of Bcl-xL on the regulation of senescence in PanINs. Collectively, Bcl-xL overexpression in PanINs promotes progression to PDAC by inhibiting apoptosis, particularly in high-grade PanINs, and oncogene-induced senescence in low-grade PanINs.

In the experiments using Bcl-xL KO P-KrasG12D mice, Bcl-xL deficiency significantly increased the number of senescent cells in PanIN-2/3 lesions from the P-KrasG12D mice (Figure 7*C*–*E*). In P-KrasG12D mice, Bcl-xL expression showed a graded increase with the progression from PanIN-1 to PDAC, whereas oncogene-induced senescence was detected frequently in PanIN-1, but rarely found in PanIN-2/3 and PDAC (Figures 1*D* and *E*, and 5*C*–*E*). Bcl-xL overexpression in PanIN-1 lesions significantly decreased the number of senescent cells (Figure 5*C*–*E*). These results suggest that the gradual increase of Bcl-xL expression suppresses senescence in PanINs. Regarding cancer cell senescence, previous studies have shown that Bcl-xL overexpression inhibits senescence by preventing reactive oxygen species generation.[46] ABT-737, a small molecule that inhibits Bcl-xL, increases senescence and reactive oxygen species levels.[47] In the present study, Bcl-xL knockdown in PDAC cell lines increased the number of senescent cells (Figure 8*C*). Collectively, Bcl-xL inhibition could induce senescence in PDAC as well as PanINs. Advanced PDAC remains difficult to treat,[48] and therapies preventing the progression of PanINs to PDAC could be promising treatments to reduce the incidence of PDAC. Treatments for Bcl-xL may be an efficient preventive therapy for patients at high risk of developing PanINs, such as patients with chronic pancreatitis.[49]

In conclusion, we clarified that Bcl-xL expression levels increase with the progression of pancreatic neoplasia from PanIN-1 to PDAC, whereas oncogene-induced senescence decreases. Bcl-xL overexpression suppresses oncogene-induced senescence in low-grade PanINs and inhibits apoptosis in high-grade PanINs, promoting the progression to high-grade PanINs and PDAC. Together with the finding that Bcl-xL deficiency in Kras mutant mice increases senescence, Bcl-xL is suggested to be an effective target for the prevention of PDAC by inducing senescence in PanINs.

References

1. Jemal A, Bray F, Center MM, Ferlay J, Ward E, Forman D. Global cancer statistics. CA Cancer J Clin 2011; 61:69–90.
2. Tang H, Partyka K, Hsueh P, Sinha JY, Kletter D, Zeh H, Huang Y, Brand RE, Haab BB. Glycans related to the CA19-9 antigen are increased in distinct subsets of pancreatic cancers and improve diagnostic accuracy over CA19-9. Cell Mol Gastroenterol Hepatol 2016; 2:210–221.
3. Siegel RL, Miller KD, Jemal A. Cancer statistics, 2016. CA Cancer J Clin 2016;66:7–30.
4. Scarlett CJ, Salisbury EL, Biankin AV, Kench J. Precursor lesions in pancreatic cancer: morphological and molecular pathology. Pathology 2011;43:183–200.
5. Basturk O, Hong SM, Wood LD, Adsay NV, Albores-Saavedra J, Biankin AV, Brosens LA, Fukushima N, Goggins M, Hruban RH, Kato Y, Klimstra DS, Klöppel G, Krasinskas A, Longnecker DS, Matthaei H, Offerhaus GJ, Shimizu M, Takaori K, Terris B, Yachida S, Esposito I, Furukawa T; Baltimore Consensus Meeting. A revised classification system and recommendations from the Baltimore consensus meeting for neoplastic precursor lesions in the pancreas. Am J Surg Pathol 2015;39:1730–1741.

6. Hruban RH, Takaori K, Klimstra DS, Adsay NV, Albores-Saavedra J, Biankin AV, Biankin SA, Compton C, Fukushima N, Furukawa T, Goggins M, Kato Y, Klöppel G, Longnecker DS, Lüttges J, Maitra A, Offerhaus GJ, Shimizu M, Yonezawa S. An illustrated consensus on the classification of pancreatic intraepithelial neoplasia and intraductal papillary mucinous neoplasms. Am J Surg Pathol 2004;28:977–987.
7. Morris JP, Wang SC, Hebrok MKRAS. Hedgehog, Wnt and the twisted developmental biology of pancreatic ductal adenocarcinoma. Nat Rev Cancer 2010;10:683–695.
8. Kanda M, Matthaei H, Wu J, Hong SM, Yu J, Borges M, Hruban RH, Maitra A, Kinzler K, Vogelstein B, Goggins M. Presence of somatic mutations in most early-stage pancreatic intraepithelial neoplasia. Gastroenterology 2012;142:730–733.e9.
9. Hingorani SRS, Petricoin EF, Maitra A, Rajapakse V, King C, Jacobetz MA, Ross S, Conrads TP, Veenstra TD, Hitt BA, Kawaguchi Y, Johann D, Liotta LA, Crawford HC, Putt ME, Jacks T, Wright CV, Hruban RH, Lowy AM, Tuveson DA. Preinvasive and invasive ductal pancreatic cancer and its early detection in the mouse. Cancer Cell 2003;4:437–450.
10. Takehara T, Tatsumi T, Suzuki T, Rucker EB 3rd, Hennighausen L, Jinushi M, Miyagi T, Kanazawa Y, Hayashi N. Hepatocyte-specific disruption of Bcl-xL leads to continuous hepatocyte apoptosis and liver fibrotic responses. Gastroenterology 2004;127:1189–1197.
11. Hikita H, Takehara T, Kodama T, Shimizu S, Hosui A, Miyagi T, Tatsumi T, Ishida H, Ohkawa K, Li W, Kanto T, Hiramatsu N, Hennighausen L, Yin XM, Hayashi N. BH3-only protein bid participates in the Bcl-2 network in healthy liver cells. Hepatology 2009;50:1972–1980.
12. Hirsova P, Gores GJ. Death receptor-mediated cell death and proinflammatory signaling in nonalcoholic steatohepatitis. Gastroenterol Hepatol 2015;1:17–27.
13. Sharma J, Srinivasan R, Majumdar S, Mir S, Radotra BD, Wig JD. Bcl-XL protein levels determine apoptotic index in pancreatic carcinoma. Pancreas 2005;30:337–342.
14. Miyamoto Y, Hosotani R, Wada M, Lee JU, Koshiba T, Fujimoto K, Tsuji S, Nakajima S, Doi R, Kato M, Shimada Y, Imamura M. Immunohistochemical analysis of Bcl-2, Bax, Bcl-X, and Mcl-1 expression in pancreatic cancers. Oncology 1999;56:73–82.
15. Aguirre AJA, Bardeesy N, Sinha M, Lopez L, Tuveson DA, Horner J, Redston MS, DePinho RA. Activated Kras and Ink4a/Arf deficiency cooperate to produce metastatic pancreatic ductal adenocarcinoma. Genes Dev 2003;17:3112–3126.
16. Kodama T, Takehara T, Hikita H, Shimizu S, Shigekawa M, Li W, Miyagi T, Hosui A, Tatsumi T, Ishida H, Kanto T, Hiramatsu N, Yin XM, Hayashi N. BH3-only activator proteins Bid and Bim are dispensable for Bak/Bax-dependent thrombocyte apoptosis induced by Bcl-xL deficiency: molecular requisites for the mitochondrial pathway to apoptosis in platelets. J Biol Chem 2011;286:13905–13913.
17. Hikita H, Kodama T, Shimizu S, Li W, Shigekawa M, Tanaka S, Hosui A, Miyagi T, Tatsumi T, Kanto T, Hiramatsu N, Morii E, Hayashi N, Takehara T. Bak deficiency inhibits liver carcinogenesis: a causal link between apoptosis and carcinogenesis. J Hepatol 2012;57:92–100.
18. Hruban RH, Adsay NV, Albores-Saavedra J, Anver MR, Biankin AV, Boivin GP, Furth EE, Furukawa T, Klein A, Klimstra DS, Kloppel G, Lauwers GY, Longnecker DS, Luttges J, Maitra A, Offerhaus GJ, Pérez-Gallego L, Redston M, Tuveson DA. Pathology of genetically engineered mouse models of pancreatic exocrine cancer: consensus report and recommendations. Cancer Res 2006;66:95–106.
19. Louhimo JM, Steer ML, Perides G. Necroptosis is an important severity determinant and potential therapeutic target in experimental severe pancreatitis. Gastroenterol Hepatol 2016;2:519–535.
20. Mareninova OA, Sendler M, Malla SR, Yakubov I, French SW, Tokhtaeva E, Vagin O, Oorschot V, Lüllmann-Rauch R, Blanz J, Dawson D, Klumperman J, Lerch MM, Mayerle J, Gukovsky I, Gukovskaya AS. Lysosome associated membrane proteins maintain pancreatic acinar cell homeostasis: LAMP-2 deficient mice develop pancreatitis. Gastroenterol Hepatol 2015;1:678–694.
21. Hikita H, Takehara T, Shimizu S, Kodama T, Li W, Miyagi T, Hosui A, Ishida H, Ohkawa K, Kanto T, Hiramatsu N, Yin XM, Hennighausen L, Tatsumi T, Hayashi N. Mcl-1 and Bcl-xL cooperatively maintain integrity of hepatocytes in developing and adult murine liver. Hepatology 2009;50:1217–1226.
22. Ohuchida K, Mizumoto K, Yamada D, Fujii K, Ishikawa N, Konomi H, Nagai E, Yamaguchi K, Tsuneyoshi M, Tanaka M. Quantitative analysis of MUC1 and MUC5AC mRNA in pancreatic juice for preoperative diagnosis of pancreatic cancer. Int J Cancer 2006;118:405–411.
23. Friess H, Lu Z, Andrén-Sandberg A, Berberat P, Zimmermann A, Adler G, Schmid R, Büchler MW. Moderate activation of the apoptosis inhibitor Bcl-xL worsens the prognosis in pancreatic cancer. Ann Surg 1998;228:780–787.
24. Debacq-Chainiaux F, Erusalimsky JD, Campisi J, Toussaint O. Protocols to detect senescence-associated beta-galactosidase (SA-betagal) activity, a biomarker of senescent cells in culture and in vivo. Nat Protoc 2009;4:1798–1806.
25. Shimizu S, Takehara T, Hikita H, Kodama T, Miyagi T, Hosui A, Tatsumi T, Ishida H, Noda T, Nagano H, Doki Y, Mori M, Hayashi N. The let-7 family of microRNAs inhibits Bcl-xL expression and potentiates sorafenib-induced apoptosis in human hepatocellular carcinoma. J Hepatol 2010;52:698–704.
26. Shigekawa M, Hikita H, Kodama T, Shimizu S, Li W, Uemura A, Miyagi T, Hosui A, Kanto T, Hiramatsu N, Tatsumi T, Takeda K, Akira S, Takehara T. Pancreatic STAT3 protects mice against caerulein-induced pancreatitis via PAP1 induction. Am J Pathol 2012;181:2105–2113.

27. Adams JM, Cory S. The Bcl-2 apoptotic switch in cancer development and therapy. Oncogene 2007;26:1324–1337.
28. Moir JAG, White SA, Mann J. Arrested development and the great escape–the role of cellular senescence in pancreatic cancer. Int J Biochem Cell Biol 2014;57:142–148.
29. Morton JP, Jamieson NB, Karim SA, Athineos D, Ridgway RA, Nixon C, McKay CJ, Carter R, Brunton VG, Frame MC, Ashworth A, Oien KA, Evans TR, Sansom OJ. LKB1 haploinsufficiency cooperates with Kras to promote pancreatic cancer through suppression of p21-dependent growth arrest. Gastroenterology 2010;139:586–597, 597.e1.
30. Korkolopoulou P, Lazaris ACh, Konstantinidou AE, Kavantzas N, Patsouris E, Christodoulou P, Thomas-Tsagli E, Davaris P. Differential expression of bcl-2 family proteins in bladder carcinomas. Relationship with apoptotic rate and survival. Eur Urol 2002;41:274–283.
31. Takehara T, Liu X, Fujimoto J, Friedman SL, Takahashi H. Expression and role of Bcl-xL in human hepatocellular carcinomas. Hepatology 2001;34:55–61.
32. Hikita H, Takehara T, Shimizu S, Kodama T, Shigekawa M, Iwase K, Hosui A, Miyagi T, Tatsumi T, Ishida H, Li W, Kanto T, Hiramatsu N, Hayashi N. The Bcl-xL inhibitor, ABT-737, efficiently induces apoptosis and suppresses growth of hepatoma cells in combination with sorafenib. Hepatology 2010;52:1310–1321.
33. Watanabe J, Kushihata F, Honda K, Sugita A, Tateishi N, Mominoki K, Matsuda S, Kobayashi N. Prognostic significance of Bcl-xL in human hepatocellular carcinoma. Surgery 2004;135:604–612.
34. Bauer C, Hees C, Sterzik A, Bauernfeind F, Mak'Anyengo R, Duewell P, Lehr HA, Noessner E, Wank R, Trauzold A, Endres S, Dauer M, Schnurr M. Proapoptotic and antiapoptotic proteins of the Bcl-2 family regulate sensitivity of pancreatic cancer cells toward gemcitabine and T-cell-mediated cytotoxicity. J Immunother 2015;38:116–126.
35. Shi M, He X, Wei W, Wang J, Zhang T, Shen X. Tenascin-C induces resistance to apoptosis in pancreatic cancer cell through activation of ERK/NF-κB pathway. Apoptosis 2015;20:843–857.
36. Hingorani SR, Wang L, Multani AS, Combs C, Deramaudt TB, Hruban RH, Rustgi AK, Chang S, Tuveson DA. Trp53R172H and KrasG12D cooperate to promote chromosomal instability and widely metastatic pancreatic ductal adenocarcinoma in mice. Cancer Cell 2005;7:469–483.
37. Ijichi H, Chytil A, Gorska AE, Aakre ME, Fujitani Y, Fujitani S, Wright CV, Moses HL. Aggressive pancreatic ductal adenocarcinoma in mice caused by pancreas-specific blockade of transforming growth factor-β signaling in cooperation with active Kras expression. Genes Dev 2006;20:3147–3160.
38. Delbridge ARD, Strasser A. The BCL-2 protein family, BH3-mimetics and cancer therapy. Cell Death Differ 2015;22:1071–1080.
39. Choi S, Chen Z, Tang LH, Fang Y, Shin SJ, Panarelli NC, Chen YT, Li Y, Jiang X, Du YC. Bcl-xL promotes metastasis independent of its anti-apoptotic activity. Nat Commun 2016;7:10384.
40. Chen D, Zheng X, Kang D, Yan B, Liu X, Gao Y, Zhang K. Apoptosis and expression of the Bcl-2 family of proteins and P53 in human pancreatic ductal adenocarcinoma. Med Princ Pract 2012;21:68–73.
41. Lüttges J, Neumann S, Jesnowski R, Borries V, Löhr M, Klöppel G. Lack of apoptosis in PanIN-1 and PanIN-2 lesions associated with pancreatic ductal adenocarcinoma is not dependent on K-ras status. Pancreas 2003;27:e57–e62.
42. Grasso D, Garcia MN, Hamidi T, Cano C, Calvo E, Lomberk G, Urrutia R, Iovanna JL. Genetic inactivation of the pancreatitis-inducible gene Nupr1 impairs PanIN formation by modulating Kras(G12D)-induced senescence. Cell Death Differ 2014;21:1633–1641.
43. Kennedy AL, Morton JP, Manoharan I, Nelson DM, Jamieson NB, Pawlikowski JS, McBryan T, Doyle B, McKay C, Oien KA, Enders GH, Zhang R, Sansom OJ, Adams PD. Activation of the PIK3CA/AKT pathway suppresses senescence induced by an activated RAS oncogene to promote tumorigenesis. Mol Cell 2011;42:36–49.
44. Guerra C, Collado M, Navas C, Schuhmacher AJ, Hernández-Porras I, Cañamero M, Rodriguez-Justo M, Serrano M, Barbacid M. Pancreatitis-induced inflammation contributes to pancreatic cancer by inhibiting oncogene-induced senescence. Cancer Cell 2011;19:728–739.
45. Yosef R, Pilpel N, Tokarsky-Amiel R, Biran A, Ovadya Y, Cohen S, Vadai E, Dassa L, Shahar E, Condiotti R, Ben-Porath I, Krizhanovsky V. Directed elimination of senescent cells by inhibition of BCL-W and BCL-XL. Nat Commun 2016;7:11190.
46. Jung MS, Jin DH, Chae HD, Kang S, Kim SC, Bang YJ, Choi TS, Choi KS, Shin DY. Bcl-xL and E1B-19K proteins inhibit p53-induced irreversible growth arrest and senescence by preventing reactive oxygen species-dependent p38 activation. J Biol Chem 2004;279:17765–17771.
47. Song JH, Kandasamy K, Zemskova M, Lin YW, Kraft AS. The BH3 mimetic ABT-737 induces cancer cell senescence. Cancer Res 2011;71:506–515.
48. Garrido-Laguna I, Hidalgo M. Pancreatic cancer: from state-of-the-art treatments to promising novel therapies. Nat Rev Clin Oncol 2015;12:319–334.
49. LeBlanc JK, Chen JH, Al-Haddad M, Luz L, McHenry L, Sherman S, Juan M, Dewitt J. Can endoscopic ultrasound predict pancreatic intraepithelial neoplasia lesions in chronic pancreatitis?: a retrospective study of pathologic correlation. Pancreas 2014;43:849–854.

Received August 2, 2016. Accepted February 9, 2017.

Correspondence
Address correspondence to: Tetsuo Takehara, MD, PhD, Department of Gastroenterology and Hepatology, Osaka University Graduate School of

Medicine, 2-2 Yamada-oka, Suita, Osaka 565 0871, Japan. e-mail: takehara@gh.med.osaka-u.ac.jp; fax: (81) 6-6879-3629.

Acknowledgments
The authors thank Dr Lothar Hennighausen (Laboratory of Genetics and Physiology, National Institute of Diabetes and Digestive and Kidney Diseases, National Institute of Health, Bethesda, MD) for providing the *bcl-x*$^{flox/flox}$ mice.

Author contributions
Study concept and design: K. Ikezawa, H. Hikita, M. Shigekawa, and T. Takehara. Acquisition of data: K. Ikezawa, M. Shigekawa, K. Iwahashi, H. Eguchi, and R. Sakamori. Analysis and interpretation of data: K. Ikezawa, H. Hikita, M. Shigekawa, T. Tatsumi, and T. Takehara. Writing, review, or revision of the manuscript: K. Ikezawa, H. Hikita, and T. Takehara.

Conflicts of interest
The authors disclose no conflicts.

Funding
This work was supported in part by grants-in-aid for Scientific Research from the Ministry of Education, Culture, Sports, Science and Technology, Japan (JP16K15429 to T.Tak. and JP25860534 and JP15k19325 to M.S.) and research grant from Bristol-Myers Squibb (to H.H.).

Supplementary Materials and Methods

Genetically Engineered Mouse Models and Mouse Strains

Mice were genotyped by polymerase chain reaction analysis. The oligonucleotide primer sequences were as follows: Kras,

5'-CCTTTACAAGCGCACGCAGACTGTAGA-3' (sense) and

5'-AGCTAGCCACCATGGCTTGAGTAAGTCTGCA-3' (antisense); Pdx1-Cre,

5'-CTGGACTACATCTTGAGTTGC-3' (sense) and 5'-GGTGTACGGTCAGTAAATTTG-3' (antisense); Bcl-xL Tg,

5'-GCTGGTTATTGTGCTGTCTC-3' (sense) and 5'-GGTAAGTGGCCATCCAAGCTGC-3' (antisense); and *bcl-x*$^{flox/flox}$,

5'-GCCACCTCATCAGTCGGG-3' (sense) and 5'-TCAGAAG-CCGCAATATCCCC-3' (antisense).